Author(s): Young, E. S. K. & Bouravleuv, A. D. & Cirlin, G. E. & Dhaka, V. & Lipsanen, Harri & Tchernycheva, M. & Scherbakov, A. V. & Platonov, A. V. & Akimov, A. V. & Kent, A. J.

Title: Electrical detection of picosecond acoustic pulses in vertical transport devices with nanowires

Year: 2014

Version: Final published version

Please cite the original version:

Young, E. S. K. & Bouravleuv, A. D. & Cirlin, G. E. & Dhaka, V. & Lipsanen, Harri & Tchernycheva, M. & Scherbakov, A. V. & Platonov, A. V. & Akimov, A. V. & Kent, A. J. 2014. Electrical detection of picosecond acoustic pulses in vertical transport devices with nanowires. Applied Physics Letters. Volume 104, Issue 6. P. 062102/1-4. ISSN 0003-6951 (printed). DOI: 10.1063/1.4864637.

AIP | Applied Physics Letters

Electrical detection of picosecond acoustic pulses in vertical transport devices with nanowires

E. S. K. Young, A. D. Bouravleuv, G. E. Cirlin, V. Dhaka, H. Lipsanen, M. Tchernycheva, A. V. Scherbakov, A. V. Platonov, A. V. Akimov, and A. J. Kent

Citation: Applied Physics Letters **104**, 062102 (2014); doi: 10.1063/1.4864637
View online: http://dx.doi.org/10.1063/1.4864637
View Table of Contents: http://scitation.aip.org/content/aip/journal/apl/104/6?ver=pdfcov
Published by the AIP Publishing

Electrical detection of picosecond acoustic pulses in vertical transport devices with nanowires

E. S. K. Young,[1] A. D. Bouravleuv,[2,3,4,5] G. E. Cirlin,[2,3,4] V. Dhaka,[5] H. Lipsanen,[5] M. Tchernycheva,[6] A. V. Scherbakov,[3] A. V. Platonov,[2,3,4] A. V. Akimov,[1,3] and A. J. Kent[1]
[1]*School of Physics and Astronomy, University of Nottingham, Nottingham NG7 2RD, United Kingdom*
[2]*St.Petersburg Academic University RAS, 195220 St.Petersburg, Russia*
[3]*Ioffe Physical Technical Institute RAS, 194021 St.Petersburg, Russia*
[4]*Spin Optics Laboratory and Physics Department, St.Petersburg State University, 199004 St.Petersburg, Russia*
[5]*Department of Micro and Nanosciences, School of Electrical Engineering, Aalto University, FI-00076 Aalto, Finland*
[6]*Institut d'Electronique Fondamentale UMR CNRS 8622, University Paris Sud 11, 91405 Orsay Cedex, France*

(Received 13 January 2014; accepted 26 January 2014; published online 10 February 2014)

Picosecond acoustic pulses, generated in a thin aluminum transducer, are injected into semiconductor vertical transport devices consisting of core-shell GaAsP nanowires. The acoustic pulses induce current pulses in the device with amplitude $\sim$1 μA. The spectrum of the electrical response is sensitive to the elastic properties of the device and has a frequency cutoff at $\sim$10 GHz. This work shows the potential of the technique for studies the elastic properties of complex semiconductor nanodevices. © *2014 AIP Publishing LLC*. [http://dx.doi.org/10.1063/1.4864637]

Since the development of the picosecond acoustic technique in 1984 by Thomsen *et al.*,[1,2] ultrashort acoustic pulses have been used to probe various nanoobjects. The wavelengths of acoustic waves in the wavepackets of picosecond acoustic pulses lie in submicrometer range, enabling information about the size and elastic properties of the objects in complex devices to be obtained with nanometer spatial resolution. Experiments have been performed where images with nanometer resolutions were obtained in various devices, including computer chips,[3] biological specimens,[4] heterointerfaces,[5] surface profiles,[6] and buried nanolayers.[7] Optoacoustic echography and interferometry on a picosecond time scale have also been successfully used for characterization of new materials for electronic devices.[8,9] In future, probing by picosecond acoustic pulses will potentially become a nanometer analog of ultrasound and photoacoustic techniques which nowadays operate at frequencies up to about 1 GHz.

For the detection of picosecond acoustic pulses, most of the studies exploit the effect of the strain on the transmission or reflection of ultrashort probe light pulses.[1,2] This technique is convenient in that the probe light pulse is derived from the same laser beam as the femtosecond pump pulse that is used to excite the picosecond acoustic pulses, and allows detection of acoustic signals with frequencies up to 2 THz. However, optical detection of picosecond acoustic pulses strongly limits the possible applications. For example: the conventional optical pump-probe technique cannot be used in the samples which do not reflect or transmit light (e.g., solar cell devices) or if the sample surface is not of optical quality. This problem could be solved by electrical detection of acoustic pulses using vertical semiconductor devices like Schottky[10] or resonant tunneling[11] diodes. In this case, the temporal resolution is limited by the frequency bandwidth of the external electrical or microwave circuits which, nowadays, can exceed 100 GHz. One of the significant advantages of using electrical detection in nontransparent materials is the possibility to embed the detector inside the complex nanostructure and get information about the acoustic field not only near the surface of the sample, as in the optical pump-probe technique, but at a certain point within the nanostructure with nanometer spatial resolution. Such a challenging proposal has not been yet realized experimentally and stands as a main motivation for the present work.

In the present paper we realize the electrical detection of picosecond acoustic pulses in a complex semiconductor structure with vertical nanowires (NWs), which has been created as a solar cell prototype. The standard picosecond acoustic pump-probe techniques cannot be used because the surface of the structures does not reflect light. We show that the electrical detection of picosecond acoustic pulses in NW devices provides 100 ps temporal resolution which is limited by the external electrical circuit. The detected signal is sensitive to the elastic properties of the complex device which is demonstrated in our work by comparison of the signals in different structures.

The experimental setup is schematically shown in Fig. 1(a). The studied structure consists of core–shell GaAsP NWs grown by Au-assisted Metal-Organic Vapor Phase Epitaxy (MOVPE) on n^+-Si(001) substrate. The detailed description of the growth procedure can be found in Ref. 12. The GaAsP n-doped core has been formed by adding disilane (Si_2H_6) during the NW growth, the p-doped GaAsP shell was formed during 10 s using diethylzinc (DEZn) as a dopant source. The alloy composition was determined from the optical measurements to be close to $GaAs_{0.82}P_{0.18}$. The diameter and the length of NWs were 320 ± 40 nm and 2.2 ± 0.2 μm, respectively. The NW density was kept intentionally low $\sim 5 \times 10^6$ cm^{-2}, and the space between the NWs was filled by SiO_x. Devices were fabricated in the form of square mesas with open top contacts. The top mesa surface was covered with 150 nm of conductive indium tin oxide (ITO) layer to contact the NW tips, and the Si substrate was used as a bottom contact. Metal contacts (10 nm Ti/150 nm Au) were then deposited on the Si substrate and on the top mesa

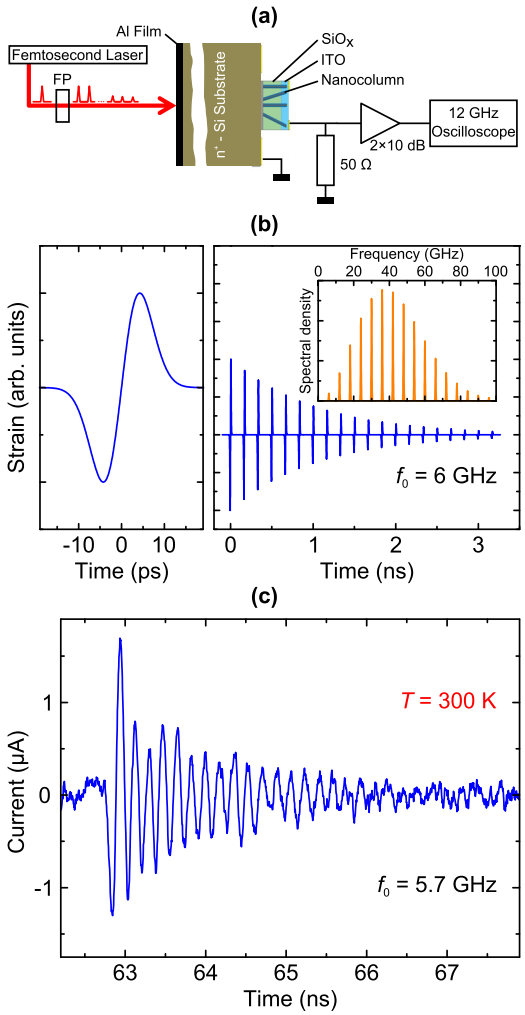

FIG. 1. (a) The scheme of the experiment. (b) The calculated temporal evolution of the single strain pulse (left panel) and the burst of strain pulses (right panel); inset shows the spectrum of the burst. (c) The temporal evolution of the electrical signal measured at room temperature in the $300 \times 300\ \mu m^2$ nanowire device.

surface, leaving the central part of the mesa open for front illumination.[12]

For the picosecond acoustic experiments, the back surface of the Si substrate was polished and a 100 nm Al acoustic transducer film was deposited on it. The total thickness of the sample after polishing was 535 μm. In the experiments, we used two mesas with dimensions 300×300 and $600 \times 600\ \mu m^2$. The samples were mounted on strip-line waveguide holders designed for measurements up to ~14 GHz and Au wires were bonded to the contacts of the devices with silver epoxy. The samples were mounted in a He-flow cryostat which allowed for carrying out both room and low temperature experiments.

Picosecond acoustic pulses were generated by the excitation of the Al transducer with pulses from a regeneratively amplified femtosecond Ti:Sapphire laser (wavelength 800 nm, pulse duration 60 fs, repetition rate 5 kHz). The beam from the laser was passed through a Fabry-Perot interferometer, labeled as FP in Fig. 1(a), which emitted at the output a burst of optical pulses with the repetition rate f_0 defined by the distance x between the mirrors of the interferometer ($f_0 = c/2x$). The reflectivity of the input and output mirrors were 95% and 90%, respectively, which results in a 15% decrease of each optical pulse relative to the previous one in the burst. The output beam, with maximum average power ~1 mW, was focused to a spot on the Al transducer with a diameter of 200 μm exactly opposite to the center of the NW device.

Each optical pulse in the excitation burst incident on the Al transducer generates an antisymmetric strain pulse illustrated in the left part of Fig. 1(b).[2] The duration of the strain pulse is ~10 ps which is much smaller than the time between the pulses in the burst (in the experiments $f_0 < 20$ GHz). Thus the burst of the optical pulses is converted into the burst of, well separated in time, strain pulses whose amplitudes are proportional to the energy of the corresponding optical pulse in the burst. The spectrum of the strain pulse burst consists of peaks centered at the frequencies $f_n = nf_0$ where $n = 1, 2, \ldots$. The amplitudes of the spectral peaks for various n are governed by the spectrum of the individual strain pulse in the burst, which extends up to ~100 GHz. The modeled profile of the strain pulse burst with $f_0 = 5$ GHz and its Fast Fourier transform (FFT) spectrum is shown in right part of Fig. 1(b).

The burst of strain pulses generated in the Al transducer is injected into the Si substrate where it propagates with the speed of longitudinal sound ($s_{Si} = 8430$ m/s at $T = 300$ K) and after a time $t_0 \approx 63$ ns reaches the NW device. The burst of pulses is detected by probing the changes of the current in the microwave circuit which includes the NW device, a 50 Ω load resistor, two 10 dB amplifiers and a 12 GHz oscilloscope [see the scheme in Fig. 1(a)]. The temporal signal $\Delta I(t)$ detected in the 300 μm device at $T = 300$ K, zero bias, and $f_0 = 5.7$ GHz is shown in Fig. 1(c). The decaying oscillations with a frequency of the first harmonic f_0 which start at $t_0 = 62.7$ ns are clearly seen. The measured signals $\Delta I(t)$ do not depend on the applied bias, and all the data presented below correspond to the zero bias experiments.

The usage of the strain pulse burst instead of a single strain pulse enables more accurate measurement of the acoustic frequency cutoff, f_c, of the electrical detection method. This is because as soon as $f_0 > f_c$ it becomes impossible to resolve the individual strain pulses and there will be no spectral components for $nf_0 > f_c$ in the FFT spectrum. To demonstrate this we performed the experiments on the 300 μm device at $T = 5$ K when $\Delta I(t)$ has an order of magnitude higher amplitude compared with $\Delta I(t)$ at $T = 300$ K. The temporal traces $\Delta I(t)$, measured for different f_0, and their FFTs are shown in Figs. 2(a) and 2(b), respectively. It is seen that the temporal resolution of the electrical detection method allows the resolution in $\Delta I(t)$ of the individual strain pulses in the burst up to $f_0 \approx 10$ GHz. For essentially higher values of f_0 the individual peaks are not resolved and the FFTs do not show the distinct spectral peak. The spectral spacing $\Delta f = f_{n+1} - f_n$ between the peaks in the FFTs (Fig. 2(b)) is in agreement with the expected spectrum of the strain pulse burst, $\Delta f = f_0$. This shows that the electrical detection technique in the NW devices has an acoustic bandwidth up to at least 10 GHz. The amplitude is maximum when $f_n \approx 4$ GHz. This is different from the expected spectrum of the incident strain pulse burst [see the inset in Fig. 1(b)] where the intensity of the spectral peaks increases up to $f = 40$ GHz.

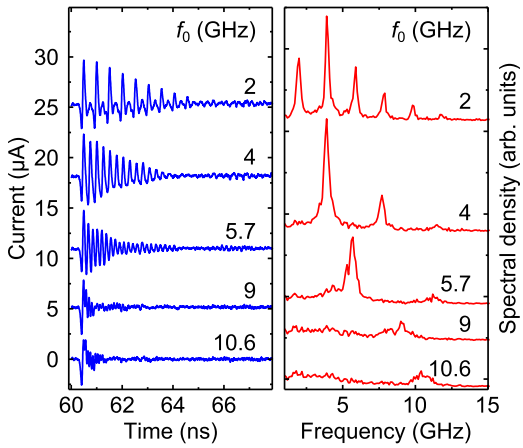

FIG. 2. Temporal evolutions of the electrical current and their Fourier spectra measured at $T = 5$ K in 300 × 300 μm^2 device for various frequencies f_0 in the strain pulse burst.

The data presented in Fig. 2 clearly demonstrate the possibility of electrical detection of picosecond strain pulses with the temporal resolution ~100 ps and corresponding acoustic frequency components up to ~10 GHz. It is most likely that the frequency cutoff $f_c \approx 10$ GHz obtained in the present work is governed by the bandwidth of the 12 GHz oscilloscope, while actually the NW device could be sensitive to higher frequencies than measured f_c.

Taking into account the complicated design of the NW device, it is difficult to specify in detail the microscopic mechanism of the electrical detection. The main conclusion which comes from the obtained value for $f_c \sim 10$ GHz is that the region of the device which is responsible for the detection has a vertical extent <250 nm. Indeed, if the whole NW device with the thickness of ~2 μm was contributing to the signal $\Delta I(t)$, then the value for f_c would be essentially less due to long (~1 ns) propagation of the strain pulse in the NW device and back to the substrate. It is therefore most probable that the detection of the strain pulses takes place at the interface between the Si substrate and the NW bases. Then the detection mechanism is based on a piezojunction effect[13,14] and is similar to the previously studied case of Schottky diodes[10] and *p-n* junctions[15] where the temporal resolution is defined by the width of the depletion layers near the interfaces. The drag of the carriers through NW by the strain pulses[16,17] in the studied devices is unlikely because of high value of f_c and respective small value of the vertical extent of the detection region.

To show that electrical detection of acoustic pulses may provide information about the elastic properties of the device we compare $\Delta I(t)$ measured in 600 μm and 300 μm devices when exciting with single picosecond strain pulses. The measured temporal traces are shown in Figs. 3(a) and 3(b) for the 600 μm and 300 μm mesas, respectively. The electrical responses are measured in the time interval between 62 and 70 ns corresponding to when the picosecond strain pulse is incident on the devices after a single passage through the Si substrate. The next responses, detected in the time interval around 190 ns, correspond to the first echo strain pulse which has traveled through the substrate two more times, following reflections at the open surfaces, before reaching the mesa. The echo signal provides useful information about the

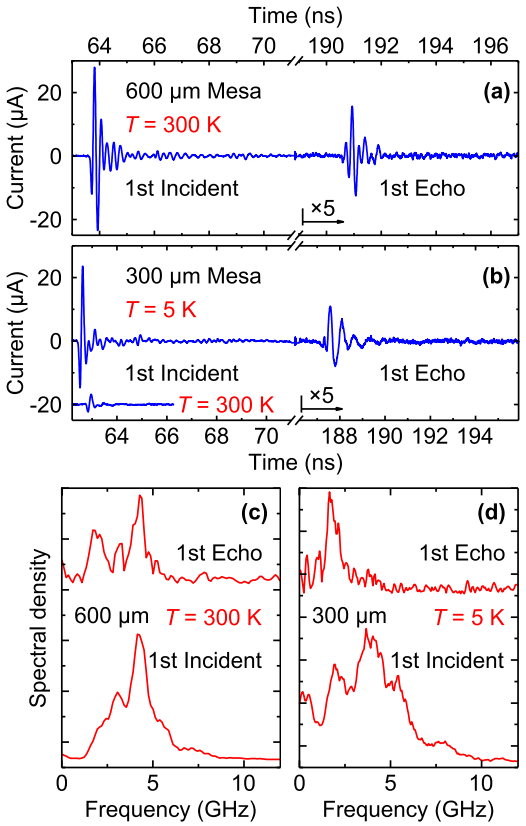

FIG. 3. Temporal evolutions (a), (b) and their Fourier spectra (c), (d) measured in 600 × 600 and 300 × 300 μm^2 devices.

acoustic reflection from the interfaces and device elements. The corresponding FFTs of the measured first incident and echo signals are presented in the insets of the corresponding panels in Figs. 3(c) and 3(d).

The differences between $\Delta I(t)$ in the two different devices are clearly seen in Fig. 3. The amplitude of $\Delta I(t)$ measured at $T = 300$ K in 300 μm device is much smaller than in the 600 μm device, so that the echo signal in 300 μm device cannot be distinguished above the noise floor. Therefore, for the 300 μm mesa we present the data obtained at low T which possesses higher amplitude of $\Delta I(t)$ without significantly changing its temporal shape. We will now compare carefully the FFT spectra of the measured signals for the two devices. First, considering the spectra of the echo signals [upper curves in Figs. 3(c) and 3(d)]. In the 600 μm device the spectrum of the echo pulse extends to frequencies in excess of 5 GHz [Fig. 3(c)]. On the other hand, in the 300 μm device the spectrum of the echo pulses possesses a cutoff at around 2 GHz [Fig. 3(d)]. This suggests that the higher frequency acoustic components are more strongly scattered and do not undergo specular reflection from the mesa back to Si substrate and thus cannot give a contribution to the echo signal.

There are also differences in the spectra of the first incident pulse obtained in the two devices [compare lower curves in Figs. 3(c) and 3(d)]. The spectral shapes possess overlapping peaks and the spacing Δf_d between these peaks is different in the two devices: $\Delta f_d = 1.2 \pm 0.2$ GHz and 1.9 ± 0.2 GHz in 600 μm and 300 μm devices, respectively. The peaks with the closer value of $\Delta f_d = 1.2$ GHz are even more pronounced in the spectrum of the echo pulse in

600 μm mesa [see the upper curve in Fig. 3(c)]. It is clear that some resonance filtering of the initially incident strain pulses takes place. This filtering may happen if the whole device behaves as a homogeneous film with mean elastic parameters[18–20] or may be due to localized vibrational modes of the device elements, e.g., extensional modes in the NWs,[21] or longitudinal vibration of the whole device. Considering the whole NW device as a homogeneous layer with the thickness d and average sound velocity s_d we get $\Delta f_d = \frac{s_d}{2d}$. Taking the values of the parameters expected from the design of the NW structure, $s_d \approx 6000$ m/s (sound velocity in SiO_x) and $d = 2.2$ μm we get, $\Delta f_d = 1.36$ GHz, which is in fair agreement with the results obtained in 600 μm device. However, the spacing of modes in the spectrum for the 300 μm device [see the lower curve in Fig. 3(b)] cannot be explained so easily by considering the vibrational modes of NWs and the various layers which form the device. Clearly, from the differences in the responses to the echo pulses, the acoustic properties of the 300 μm and 600 μm devices are quite different. This may be referred to differences in the elastic properties of the device elements and/or the quality of the interfaces introduced when the devices were contacted and mounted. Another reason for the observed effects could be a frequency-dependent transfer characteristic of the microwave circuit, which manifests itself as a "ringing" of the electrical signal following the initial impulse. This could be different for the two devices due to differences in their complex impedance related to the dimensions. These concerns do not allow us to make very definite conclusions about the elastic spectrum of the device. However, if electrical ringing effects were the dominant effect, the incident and echo pulses would be expected to have different amplitudes, but the same temporal signature, which is clearly not the case in the results presented here.

In conclusion, we have detected electrically picosecond acoustic pulses with a temporal resolution ~100 ps in semiconductor device consisting of nanowires. The method is sensitive to the elastic properties of the device and may be used in future to obtain information about the size and elastic properties of various nanoobjects in complex semiconductor devices. The basic mechanism of electrical detection is the piezojunction effect, which takes place at the interfaces of two different materials (heterojunction) or materials with different doping (e.g., *p-n* junction), where the electric field potential is sensitive to the strain. Electrical detection of picosecond acoustic pulses provides an alternative to the, widely used nowadays, optical detection technique, particularly in the case of devices which do not reflect or transmit light.

The authors acknowledge the UK Engineering and Physical Sciences Research Council, RFBR (Grants Nos. 14-02-01244-a and 13-02-12031-ofi-m) and FP7 EU "FUNPROBE" financial support.

[1]C. Thomsen, J. Strait, Z. Vardeny, H. J. Maris, J. Tauc, and J. J. Hauser, Phys. Rev. Lett. **53**, 989 (1984).
[2]C. Thomsen, H. T. Grahn, H. J. Maris, and J. Tauc, Phys. Rev. B **34**, 4129 (1986).
[3]H. J. Maris, Sci. Am. **278**, 86 (1998).
[4]C. Rossignol, N. Chigarev, M. Ducousso, B. Audoin, G. Forget, F. Guillemot, and M. C. Durrieu, Appl. Phys. Lett. **93**, 123901 (2008).
[5]S. H. Lee, A. L. Cavalieri, D. M. Fritz, M. C. Swan, R. S. Hegde, M. Reason, R. S. Goldman, and D. A. Reis, Phys. Rev. Lett. **95**, 246104 (2005).
[6]K.-H. Lin, C.-T. Yu, S.-Z. Sun, H.-P. Chen, C.-C. Pan, J.-I. Chyi, S.-W. Huang, P.-C. Li, and C.-K. Sun, Appl. Phys. Lett. **89**, 043106 (2006).
[7]K.-H. Lin, C.-M. Lai, C.-C. Pan, J.-I. Chyi, J.-W. Shi, S.-Z. Sun, C.-F. Chang, and C.-K. Sun, Nat. Nano **2**, 704 (2007).
[8]A. M. Lomonosov, A. Ayouch, P. Ruello, G. Vaude, M. R. Baklanov, P. Verdonck, L. Zhao, and V. E. Gusev, ACS Nano **6**, 1410 (2012).
[9]F. Xu, L. Belliarda, D. Fournier, E. Charron, J.-Y. Duquesne, S. Martin, C. Secouard, and B. Perrin, Thin Solid Films **548**, 366 (2013).
[10]D. M. Moss, A. V. Akimov, B. A. Glavin, M. Henini, and A. J. Kent, Phys. Rev. Lett. **106**, 066602 (2011).
[11]E. S. K. Young, A. V. Akimov, M. Henini, L. Eaves, and A. J. Kent, Phys. Rev. Lett. **108**, 226601 (2012).
[12]M. Tchernycheva, L. Rigutti, G. Jacopin, A. de Luna Bugallo, P. Lavenus, F. H. Julien, M. Timofeeva, A. D. Bouravleuv, G. E. Cirlin, V. Dhaka, H. Lipsanen, and L. Largeau, Nanotechnology **23**, 265402 (2012).
[13]H. Hall, J. Bardeen, and G. Pearson, Phys. Rev. **84**, 129 (1951).
[14]W. Rindner and E. Pittelli, J. Appl. Phys. **37**, 4437 (1966).
[15]D. M. Moss, A. V. Akimov, R. P. Campion, and A. J. Kent, Chin. J. Phys. **49**, 499 (2011).
[16]D. R. Fowler, A. V. Akimov, A. G. Balanov, M. T. Greenaway, M. Henini, T. M. Fromhold, and A. J. Kent, Appl. Phys. Lett. **92**, 232104 (2008).
[17]M. Möller, A. Hernández-Mínguez, S. Breuer, C. Pfüller, O. Brandt, M. M de Lima, Jr., A. Cantarero, L. Geelhaar, H. Riechert, and P. V. Santos, Nanoscale Res. Lett. **7**, 247 (2012).
[18]A. V. Akimov, E. S. K. Young, J. S. Sharp, V. Gusev, and A. J. Kent, Appl. Phys. Lett. **99**, 021912 (2011).
[19]H. Sun, V. A. Stoica, M. Shtein, R. Clarke, and K. P. Pipe, Phys. Rev. Lett. **110**, 086109 (2013).
[20]C. Mechri, P. Ruello, and V. Gusev, New J. Phys. **14**, 023048 (2012).
[21]P.-A. Mante, H.-P. Chen, Y.-C. Wu, C.-Y. Ho, L.-W. Tu, J.-K. Sheu, and C.-K. Sun, AIP Conf. Proc. **1506**, 2 (2012).